

A Study on Design and Optimization of High Power Density PMSM for Pod Propulsion System

Ioannis D. Chasiotis, *Student Member, IEEE*, and Yannis L. Karnavas, *Member, IEEE*

Abstract -- Pod propulsion systems are widely used in marine industry, since they exhibit high efficiency and reliability especially when they are combined with permanent magnet synchronous motors (PMSMs). A motor of this type can easily present high power density ratings in high-speed operation. However, when such a low-speed application is considered the achievement of high power density for the motor is not an easy task. Also, there is a large amount of constraints that have to be fulfilled. This paper deals with the effective design and optimization procedure of a PMSM with surface mounted magnets, which is going to be the propulsion motor of a passenger ferry. For this purpose, an appropriate objective function has been constructed and various constraints related with motor's dimensions, the maximum acceptable current density, the non-saturable operation and other practical aspects have been taken into account. Finally, the presented results are compared with others found in technical literature and reveal a quite satisfactory enhancement of motor's power density.

Index Terms--design optimization, finite element analysis, high efficiency, high power density, permanent magnet synchronous motor, pod propulsion system.

I. INTRODUCTION

SINCE the early 20th century electrical machines have been employed in cruise ships, ferries, yachts, battle ships, icebreakers, shuttle tankers, special purpose vessels, research vessels (e.g. for oceanographic explorations), etc. [1]. They have been used so far either as parts of ship's auxiliary systems or as the prime mover of the propeller. Nowadays, integrated electric ships are becoming common throughout the commercial marine industry [2]. The electric propulsion of ships is a very active and fast-growing research area driven by rapid growth in power electronics and the advancement in machine design [3]. This prospect leads to important environmental benefits considering the fuel consumption reduction, while simultaneously it offers significant advantages in efficiency, performance at low speed, maneuverability, safety and plant flexibility compared to the conventional diesel-mechanical systems [4].

The latest trend in ship propulsion is the podded propulsor, in which the prime mover is located outside of the ship's hull and mounted in an Azimuthing pod, as shown in Fig. 1. The pod system eliminates the need of a gearbox and allows the propeller to be directly mounted to the electric motor. The replacement of mechanical coupling between these two components contributes to considerable savings in space and power consumption, increases system's efficiency and reliability and improves the ship's handling during the

navigation in shallow water and embarkation/disembarkation phases [5]. Furthermore, it provides a high comfort class rating to the ship's crew and passengers due to the reduction of vibration and noise [6].

Among the most crucial decisions for the development of a pod propulsion system is the selection of electric motor's type and its topology. The motor has to exhibit high efficiency, low torque ripple and fulfill the increased requirements of power and torque density. Regarding the last mentioned feature, various structures, such as induction motors (IMs) [7,8], permanent magnet synchronous motors (PMSMs) [9,10], high temperature superconducting motors (HTSMs) [11,12] and acyclic homopolar motors [13], have been investigated and compared to each other in recent studies. Homopolar motors are low-voltage and high current devices and thus cannot easily be used in such an application. A HTSM can exhibit a power density almost twice than the corresponding one of an induction motor of the same size and over 25% higher than the one achieved by a PMSM [14]. However, the cost of superconducting materials is currently prohibitive. Thus, taking into account the great advantage of PMSMs over IMs [15], it seems that they are the most suitable choice for a pod propulsion system.

Multi-phase and high speed PMSMs can reach power density in range of 6-12 kW/kg [16]. However, a multi-phase supply system is not a common practice in commercial electric ships [17]. Moreover, the operating speed of the motors installed in vessels with direct-drive propulsion system is usually in range of 100-500 rpm and 650-1800 rpm for low and high speed ships respectively [18]. Conventional PMSMs with a small number of poles can achieve about 0.3 to 0.5 kW/kg, while the power density of PMSMs with a large poles number can be equal to 1.5 kW/kg. This relatively high power density is achievable when the motor can obtain a large diameter compared to its length [19]. However, this requirement cannot actually be met in a typical pod structure, as it can be seen from Fig. 1. A review in the relevant technical literature of the major pod systems manufacturers,

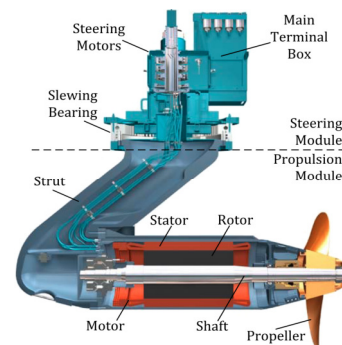


Fig. 1. The basic components of a pod propulsion system.

I. D. Chasiotis and Y.L. Karnavas are with the Electrical Machines Laboratory, Department of Electrical and Computer Engineering, Democritus University of Thrace, Xanthi, GR-67100, Hellas (e-mail: ichasiot@ee.duth.gr, karnavas@ee.duth.gr).

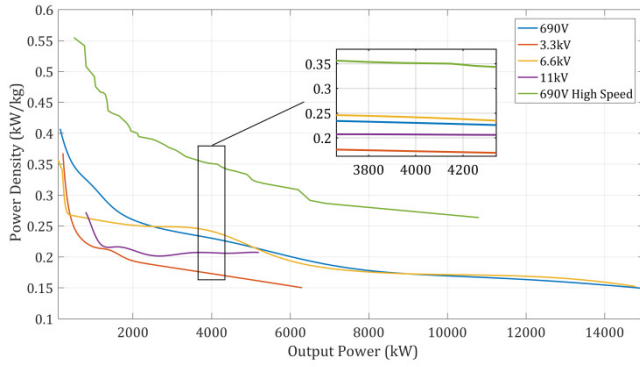


Fig. 2. The maximum power density presented by motors which are already installed in commercial electric ships with a direct-drive propulsion system.

such as ABB, Rolls Royce–Converteam, Siemens–Schottel, Wartsila SAM Electronics, GE Power Conversion, General Dynamics Electric Boat and etc. confirmed the low power density ratings of the already installed motors. Through the extended literature review the authors collected data about the power density that the aforementioned motors present. The derived results are given in Fig. 2. It is clear that there is a strong “connection” among the maximum achievable power density, the motor’s output power, the rotational speed and the level of the supply voltage.

On the basis of the above, this study aims to investigate if the power density of a PMSM can be further increased when it is to be used as a propulsion motor in a pod system of a low-speed ferry. For this purpose, on a first step (described in Section II) the ship’s propeller characteristics are determined through the conduction of parametric analysis and by taking into account the ship’s thrust requirements. Next, its configuration is optimized in order to guarantee its high efficiency and the motor’s rated power and torque are estimated. In Section III, the adopted PMSM’s design optimization algorithm is presented first and the relevant incorporated constraints, the constant quantities and the proposed objective function are thoroughly described. The corresponding results are given in Section IV and a discussion is also made regarding the overall performance of the motor topology. Finally, Section V summarizes and concludes the work.

II. PROPELLER DESIGN PROCEDURE

The main selection criteria for a passenger vessel propulsion motor are typically the maximum rotational speed of the propeller and the vessel’s speed. Notwithstanding this consideration, there are a lot of specifications that have to be estimated in order to match the motor’s power and shaft speed with the size of the vessel and an appropriately designed propeller. The propeller has to generate adequate thrust, while at the same time it should exhibit a high efficiency. The motor’s torque and power can be calculated after the determination of the geometrical parameters and the performance characteristics of the propeller. The relationship among the above quantities is described by (1) and (2), where Q_B is the torque provided by the propeller in kNm, k_Q is the torque coefficient, ρ is the fluid density in kg/m^3 , n is the rotational speed in rps, D is the propeller’s diameter in m and

P_B is the power required to drive the propeller in kW. Since in our study a direct-drive propulsion system is examined, the quantities that are calculated by the following equations are equal to motor’s output torque and power respectively.

$$Q_B = k_Q \rho n^2 D^5 \quad (1)$$

$$P_B = 2\pi n Q_B \quad (2)$$

The design procedure of a fixed-pitch propeller is not trivial. There are many factors that should be kept in mind so as to guarantee the high efficiency of the overall propulsion system. Parameters, such as the number of blades, the rotational speed and the propeller diameter have to be carefully selected. For instance, 2-6 blades can be used for the construction of the propeller. The small number of them benefits the efficiency. On the other hand, propellers with only 2 or 3 blades are not suitable for the propulsion of large passenger ferries, as in our case, since they are subjected to heavy loads. Regarding the rotational speed, a low speed usually increases the propulsive efficiency up to 15%. For low-speed vessels (i.e. under 35 knots) it is a common practice to reduce the rotational speed and increase the diameter of the propeller in order to obtain higher torque for a given power plant [20]. The diameter seems to be a crucial characteristic in determining the amount of: a) the power that a propeller can absorb and b) the thrust that is available for propulsion. Furthermore, this geometrical feature imposes several design constraints related with the pod structure and the motor dimensions. These constraints are going to be explained in Section III.

Taking the above into consideration, the propeller design and optimization procedure, which is presented in Fig. 3, has been followed in order to specify its final topology. The first step of the adopted methodology includes the determination of: a) the vessel’s speed, b) the required thrust and c) the dimensions of the propeller’s hub. For the examined here case, the ship’s speed has been set equal to 10 m/sec, while the required thrust of a passenger ferry is assumed to be equal to 300 kN. The hub’s diameter should be as small as possible in order to obtain the maximum thrust. However, there is a tradeoff between the size and the strength. A too small hub will not be able to guarantee an overall robust structure. At this initial point, the specific geometrical feature has been considered equal to 0.7 m.

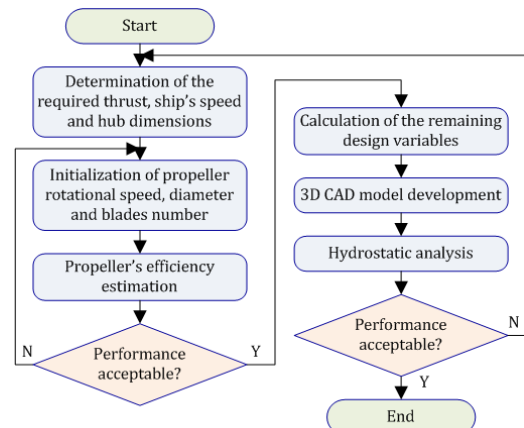


Fig. 3. Propeller's design and optimization procedure flowchart.

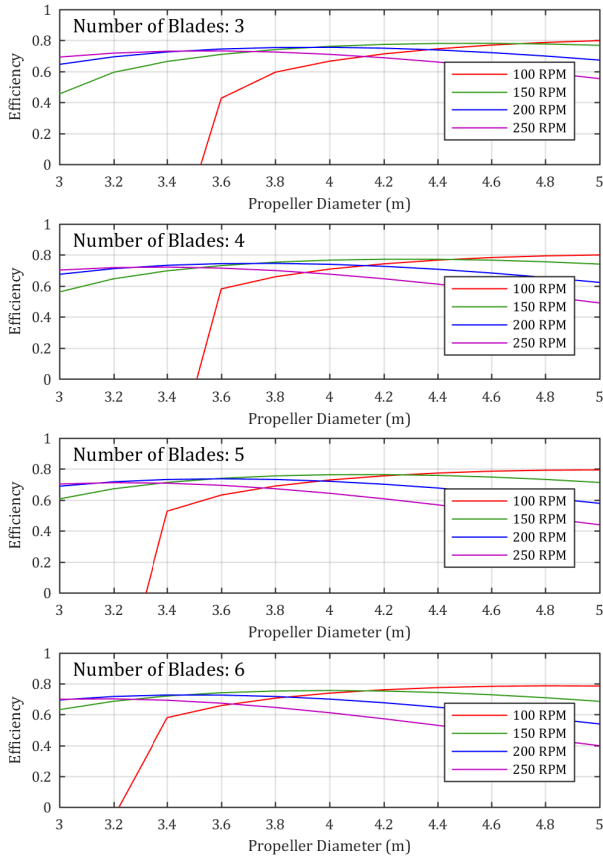


Fig. 4. Propeller's efficiency variation as a function of its rotational speed, diameter and number of blades.

Afterwards, the conduction of a parametric analysis is following. This procedure is necessary for the selection of the propeller's speed and diameter as well as its blades number. At each step of this parametric analysis the efficiency of the propeller and its hydrodynamic curve were estimated using an open-source software which is called OpenProp. The variation of propeller's efficiency as a function of the three above parameters is given in Fig. 4. By observing the derived results the following can be concluded: a) the rotational speed of 250 rpm leads to the lowest efficiency for each one of the examined cases and could be excluded from the next steps of the adopted procedure, b) the selection of 100 rpm as the propeller's speed makes sense only when its diameter is larger than 4.4 m and c) the maximum achievable efficiency when 5 or 6 blades are used is very close to the corresponding ones obtained when 3 and 4 blades are used and consequently these two cases could also be excluded.

Next, for each one of the remaining cases (i.e. three different speeds with 3 or 4 blades) the diameter value that maximized the propeller's efficiency was selected. Then, for a given diameter the rest design variables (e.g. the blade outline, the leading edge, the trailing edge, etc.) were calculated through an optimization process which was completed when the propeller's overall high performance was guaranteed. After that step, the 3D model of each derived propeller configuration was created by using a CAD software and finally hydrostatic analysis was performed for all of them. The above approach revealed that the propellers with 3 blades were subjected to a large amount of hydrostatic pres-

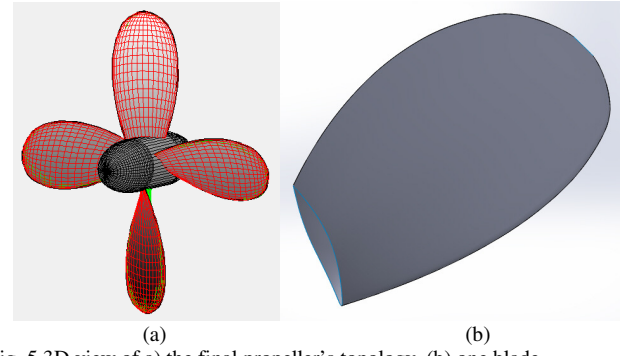


Fig. 5. 3D view of a) the final propeller's topology, b) one blade.

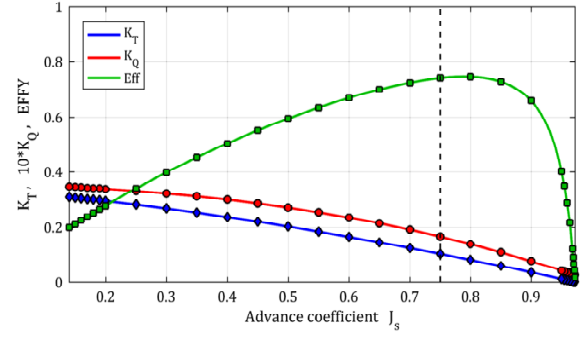


Fig. 6. The hydrodynamic curve of the selected propeller topology.

sure and consequently they had to be excluded. The final choice was a propeller with 4 blades, 4 m diameter and 200 rpm rotational speed. A 3D view of its topology is depicted in Fig. 5. The hydrodynamic curve of the selected propeller topology is also given in Fig. 6. In this curve the thrust coefficient (K_T), the torque coefficient ($10 \times K_Q$) and the propeller's efficiency ($EFFY$) are represented as a function of the advance coefficient (J_s). At its nominal operation point (marked in the specific curve) the designed propeller exhibits an efficiency of 74%, which is quite satisfactory.

III. PMSM DESIGN AND OPTIMIZATION PROCEDURE

A. Problem Specifications and Design Variables

In the examined here case, the required motor output power is equal to 4.054 MW and a torque of 193.58 kNm has to be delivered to the propeller at a speed of 200 rpm. The PMSM which is going to be designed and optimized must exhibit high efficiency (i.e. over 95%) according to the latest trends for motors with super-premium efficiency. Its nominal power factor has to be at least equal to 0.95. This feature is essential, as the propulsion motors have great effect on the ship's overall power system performance, as already stated in [21]. Additionally, the motor has to present low back-emf harmonic content, non-saturable operation, acceptable temperature behavior, low cogging torque and ripple.

Several research efforts have so far succeeded to fulfill the majority of the above requirements (e.g. [22], [23]) when a PMSM with inner rotor topology, surface mounted permanent magnets and concentrated winding has been used for low speed applications, such as a pod propulsion system. However, the various physical and practical constraints that are imposed by this application are not thoroughly clarified and incorporated in the already published scientific work.

In this study, as many constraints as possible were implemented in a simple but effective enough design and optimization methodology in order to address more adequately this specific problem. The main direction of the adopted procedure is to develop PMSMs with enhanced power and torque density, while at the same time a high overall performance will be achieved.

The followed process is depicted in a flowchart chart scheme in Fig. 7. The first step includes the estimation of the main design problem variables. In our case, these parameters are: a) the stator inner diameter (D_s), b) the motor's axial length (L), c) the permanent magnets thickness (l_m) and the current density (J_s). These four variables have to be computed (optimized) by the applied algorithm. The initialization of crucial parameters, such as the poles/slots number, the pole arc to pole pitch ratio, the airgap length and etc. follows. The other geometrical quantities, which are represented in Fig. 8 can be derived though the aforementioned variables. Reader can refer to [24] in order to find more information about the equations that were used for the calculation of these parameters. The calculation of both the magnetic (e.g. flux density estimation in the airgap, stator teeth and stator/rotor yoke, etc.) and electrical properties (e.g. induced voltage, number of turns per phase, wire diameter, etc.) has to be conducted next. Then the estimation of motor performance is conducted by determining each type of loss, the efficiency, the power factor, the total weight and the achievable power and torque density. It must be mentioned that the motor mechanical losses has been set equal to 1% of its rated output power. Finally, the performance of magnetostatic analysis using finite element method is indispensable in order to find out if any of the applied constraints is violated. If this happens, the main design variables have to be reconsidered and the algorithm process returns to its initial step. The procedure terminates when all the problem constraints and requirements are satisfied, the objective (cost) function has been minimized and no better solution can be found.

B. Problem Constants and Constraints

Regarding the materials used for the different motor's parts a high quality silicon steel has been selected for both stator and rotor core following the instructions of NEMA and IEC. Specifically, the steel M36 with a lamination thickness of 0.5 mm has been chosen. Moreover, high energy NdFeB magnets have been selected, as they have been proven efficient and reliable enough for such an application. NdFeB35 is a commercially available grade with a value of remanent flux density of 1.23 T and with large negative coercive force to prevent any potential demagnetization. The electromechanical and magnetic properties of the used materials have been considered as constants during the optimization process and they are gathered in Table I.

The applied constraints can be divided in four different categories, as they are related with electrical, physical, mechanical and magnetic features. The first group refers to electrical quantities, such as the line to line supply voltage, the frequency, the maximum current at nominal operation and the maximum acceptable current density.

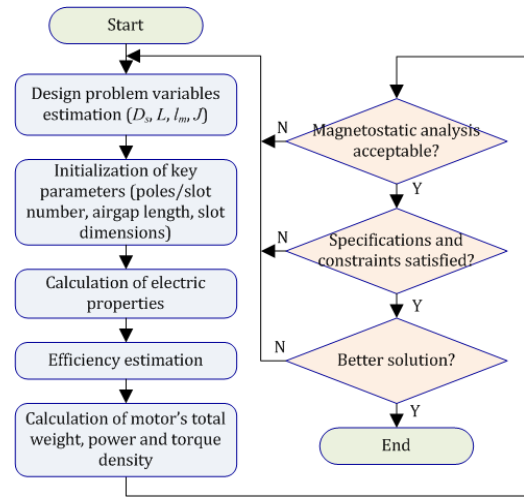


Fig. 7. Proposed overall PMSM design and optimization procedure.

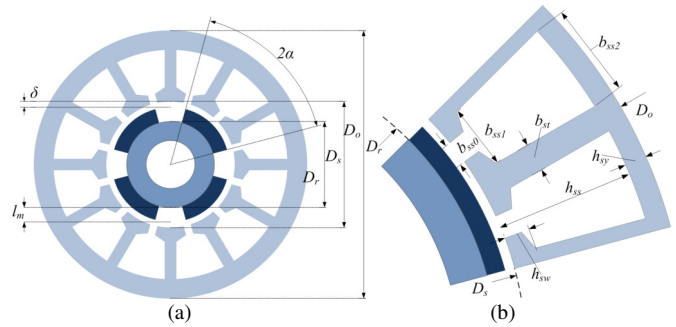


Fig. 8. Geometrical representation for the examined PMSM design, a) cross section of the whole motor, b) detailed view of the stator slots.

Generally, there are four supply voltage levels (i.e. 690 V, 3.3 kV, 6.6 kV and 11 kV) which are commonly used in commercial electric ships. However, for small and medium size ferries the most common level is 690 V according to [25]. In addition, the frequency must be as low as possible in order to reduce the motor core losses. Thus, the upper bound for this parameter has been set equal to 150 Hz. The specific choice imposes that the search space for poles number ($2p$) varies between 20 and 90 poles. Furthermore, there is a current limit set by the properties of the inverter, which specifies the amount of the motor's maximum absorbed current. In this study, this limit has been chosen to be equal to 4.5 kA taking into account the inverters characteristics used to drive motors with the same output power. Also, it is a common practice in marine industry not to utilize a cooling arrangement when PMSMs with the specific supply voltage are used in pod propulsion systems. The motor must be cooled directly by the seawater which surrounds the pod structure. Consequently, the maximum acceptable current density has been considered not to exceed 3.5 A/mm^2 , which is a quite reasonable value for a totally enclosed motor.

The second group concerns physical constraints which are related to the limited space that the application imposes. For instance, the extended technical literature review revealed that motor's outer diameter (D_o) to propeller's diameter (D) ratio varies between 0.38 and 0.54. At the same time, the motor's total axial length L (including the length of the end-windings) should not be higher than 2.60 m when the specific type of vessel is considered. The aforementioned constraints

TABLE I
CONSTANTS VALUES INCLUDED IN THE OPTIMIZATION PROCEDURE

Quantity	Symbol	Value
Magnet density	ρ_m	7400 kg/m ³
Remanence flux density	B_r	1.23 T
Magnet relative permeability	μ_r	1.09
Copper density	ρ_{cu}	8930 kg/m ³
Copper resistivity at 20° C	r_{cu}	1.68 x 10 ⁻⁸ Ωm
Steel density	ρ_s	7650 kg/m ³
Steel resistivity	r_s	4.4 x 10 ⁻⁷ Ωm

are essential for the slim and hydrodynamically optimized pod design and they have been put in place in the proposed methodology. A possible violation of the above requirements would significantly reduce the overall propulsion system's efficiency as a smooth flow of the seawater will be not achievable from now on.

The next step of constraints deals with the mechanical robustness of the machine and its manufacturing feasibility. The stator slots should be large enough to accommodate a large amount of copper and an insulation of 1.22 mm thickness which is going to be inserted as slot liner (specifications for insulation of class F had been taken into account). At the same time, the stator teeth should not be too thin. Moreover, the conductors must be geometrically possible to be placed in the slots. The round copper wires are radially inserted through the slot opening in conventional motors. Therefore, the slot opening width (b_{s0}) has to be larger than the diameter of the used round wires. A relative large b_{s0} has negative effect on the cogging torque and the flux leakage and should be avoided [26]. On the other hand, rectangular wires can be combined with a smaller slot opening width than the round ones and seem to be a more suitable choice in our case in which conductors with multi-wires are going to be used. The current technology and several winding techniques enable the easy manufacturing and the proper arrangement correspondingly of enameled rectangular copper windings with maximum width of 20 mm and maximum thickness of 5.6 mm [27]. Furthermore, configurations with single layer winding have been selected to be investigated in this context. Despite the advantages of a double layer winding, in the case of a single layer winding a higher slot fill factor can be achieved. In order to address the above issues, various constraints related with the slot geometrical parameters, such as the tooth tip height (h_{sw}), the slot opening with (b_{s0}), the slot with at the top (b_{ss2}) and others, have been set. Likewise, various design constraints, such as the minimum stator and rotor yoke height, had been taken into account in order to ensure that no saturation will occur on these parts of the motor. The maximum flux densities on other motor's parts were also specified. The design variables with their range and all the described in this Section constraints and requirements are summarized in Table II.

C. Objective (Cost) Function Formulation

Numerous objective functions have been constructed and tested in order to investigate which one addresses more adequately the specific optimization problem. Finally, the adopted function is a weighted sum of various performance indexes which are of great concern. For the examined case, it

TABLE II
OPTIMIZATION PROBLEM CONSTRAINTS AND DESIGN VARIABLES RANGE

Quantity	Symbol	Value
Efficiency	η	$\geq 95\%$
Power factor	$\cos\phi$	≥ 0.95
Max. supply voltage	V_{LL}	690
Nominal frequency	f	≤ 150 Hz
Number of poles	$2p$	20-90
Slots per pole per phase	S_{pp}	0.001-1
Nominal current	I	≤ 4.50 kA
Current density	J_s	≤ 3.5 A/mm ²
Stator outer diameter	D_o	$0.38D \leq D_o \leq 0.54D$
Motor's axial length	L	≤ 2.60 m
Stator yoke height	h_{sy}	$h_{sy} \geq 2h_{ss}/3$
Slot width at the top	h_{ss}	$0.15h_{ss} \leq b_{ss2} \leq 0.80h_{ss}$
Stator tooth tip height	h_{sw}	$h_{sw} \geq 3.50$ mm
Slot opening width	b_{s0}	≥ 6 mm
Magnet thickness	l_m	5-20 mm
Airgap length	δ	3-10 mm
Flux density in stator yoke	B_{sy}	≤ 1.8 T
Flux density in stator teeth	B_{st}	≤ 1.8 T
Flux density in rotor yoke	B_{ry}	≤ 1.8 T
Flux density in airgap	B_δ	≤ 1.0 T

is essential to enhance the power and the torque density and simultaneously to achieve high efficiency. Consequently, the proposed function is formulated as:

$$CF = \beta_1 M_{tot} + \beta_2 (1 - \eta) + \beta_3 \left(\frac{T}{I} \right) \quad (3)$$

where M_{tot} is the motor's total mass, η is the efficiency, T is the output torque, I is the current and β_{1-3} are the function's weights coefficients. The above function can be written in simple general form as $CF = \beta_i Q_i$, where β_i is a $1 \times i$ row matrix containing the weights coefficients and Q_i is an $i \times 1$ column matrix containing the quantities under optimization. A semi-exhaustive search was done first in order to explore the range values of each one of the involved quantities and determine the corresponding weight coefficient. The particle swarm optimization (PSO) method was utilized next for the minimization of the objective function. The PSO is well-known robust stochastic evolutionary technique which is based on the swarm's movement and intelligence. Reader can refer to [28] for further information about how this method is applied in electromagnetic optimization problems.

IV. DERIVED RESULTS AND DISCUSSION

The PSO has run with a swarm of 200 particles and 100 iterations. Thus, 20000 candidate configurations were investigated in order to find the optimal one. The adopted algorithm succeeded to converge to an optimal design satisfying all the applied constraints. The design variables of the proposed PMSM topology are summarized in Table III.

Compact information about its performance characteristics can be found in Table IV. The motor's total weight is equal to about 15 tons, which results to a power density of 0.2695 kW/kg. This value is higher than the corresponding one presented by the already installed motors with the same output power according to the data provided in Fig. 2. An increment of about 17.1% has been achieved and the followed design and optimization procedure seems to fulfill its main goal, i.e. the enhancement of the power density. A quite satisfactory torque density of 54.5 Nm/A has also been achieved. Simultaneously, the motor exhibits an efficiency

Quantity	Symbol	Value
Stator outer diameter	D_o	1815 mm
Stator inner diameter	D_s	1573.63 mm
Rotor outer diameter	D_r	1521.63 mm
Motor axial length	L	2280 mm
Number of poles	$2p$	56
Number of slots	Q_s	60
Airgap length	δ	8 mm
Slot opening width	b_{s0}	35 mm
Slot width at the base	b_{ss1}	41.52 mm
Slot width at the top	b_{ss2}	52 mm
Stator tooth tip height	h_{sw}	4 mm
Slot height	h_{ss}	69 mm
Stator average tooth width	b_{st}	39.46 mm
Stator yoke height	h_{sy}	50.685 mm
Rotor yoke height	h_{sr}	59.815 mm
Magnet height	h_m	18 mm
Pole arc/pole pitch ratio	$2a$	0.8
Slot fill factor	s_f	0.65
Number of turns per phase	n_c	10
Winding factor	k_w	0.951

Quantity	Symbol	Value
Nominal output power	P_{out}	4.054 MW
Maximum output power	$P_{out,max}$	6.875 MW
Nominal speed	n	200 rpm
Nominal output torque	T	193.58 kNm
Nominal current	I	3.551 kA
Current density	J_s	2.53 A/mm ²
Efficiency	η	97.77 %
Copper losses	P_{cu}	27.592 kW
Core losses	P_{core}	24.697 kW
Mechanical losses	P_{mec}	40 kW
Power factor	$\cos\phi$	0.976
Torque angle	T_{ang}	34.95 deg
Torque ripple	T_{rip}	0.4 %
Cogging torque	T_{cog}	7.05 Nm
Motor total mass	M_{tot}	15040.8 kg
Power density	P_d	0.2695 kW/kg
Torque density	P_T	54.50 Nm/A

and a power factor of 97.77% and 0.976 respectively which meets the increased requirements imposed by the marine industry and taken into account in this study. Moreover, the amount of current that the motor absorbs at its nominal operation results to a current density of 2.53 A/mm². The above low value combined with the motor's high efficiency and consequently the low heat sources indicates that adequate temperature alleviation can be occurred without the installation of a cooling system. A quite satisfactory temperature behavior could be easily achieved as the motor will be cooled by the surrounding whose temperature will be kept low directly by the seawater.

Furthermore, the motor's performance analysis using the finite element method revealed that the obtained airgap flux density and the phase back-emf (depicted in Fig. 9) present a quite sinusoidal form and very low harmonic content. The small amplitude of the odd harmonics of the phase back-emf resulted in a low value for motor's torque ripple. The specific quantity has been calculated to be equal to 0.4%. Additionally, the maximum amplitude of the cogging torque has been estimated to be equal to 7.05 Nm, which can be considered as a very low value compared to the nominal torque. Taking the above into consideration, it seems that the

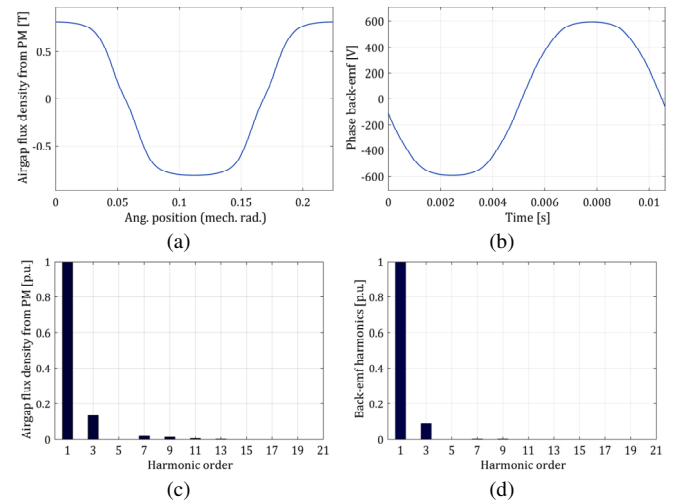


Fig. 9. Results of the proposed PMSM, a) airgap flux density, b) phase back-emf and c), d) their corresponding harmonics.

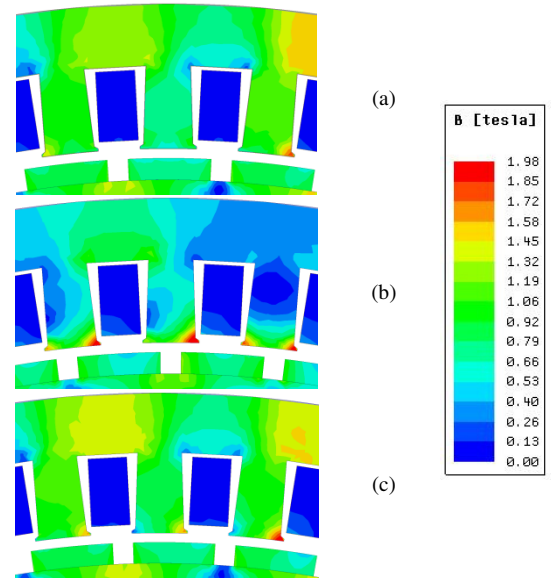


Fig. 10. Flux density distribution when a) magnet center is aligned with the stator's tooth, b) stator's tooth center is between two adjacent magnets and c) magnets edge is aligned with the tooth's tip.

motor will be free from vibrations and noise during its operation. Also, a non-saturable operation has been observed. The value of flux density developed over the different motor parts of the derived topology have been found within the acceptable limits, as it can be seen from Fig. 10.

V. CONCLUSIONS

In this study, the design and optimization procedure of a PMSM, which was to be used in a pod propulsion system, was presented and thoroughly discussed. Firstly, taking into account the ship's requirements the propeller's configuration was optimized in order to guarantee its high performance and consequently an efficient overall propulsion system. Next, plenty constraints related with the motor's characteristics and also imposed by the practical features of the specific application were analyzed and incorporated in the adopted methodology. Despite the strict constraints, an optimal PMSM topology with enhanced power density compared to

the corresponding one of the already installed motors was derived from the utilization of an appropriately formulated objective function. Finally, the finite element analysis revealed that the motor presents high efficiency and power factor, non-saturable operation, low current density, cogging torque and torque ripple.

VI. REFERENCES

- [1] J.L. Kirtley, A. Banerjee, S. Englebreton, "Motors for ship propulsion", *IEEE Proceedings*, vol. 103, issue 12, pp. 2320-2332, Dec. 2015.
- [2] T.J. McCoy, "Electric ships: past, present, and future", *IEEE Electrification Magazine*, vol. 3, issue 2, pp. 4-11, June 2015.
- [3] C. Bruzzese, "A high absolute thrust permanent magnet linear actuator for direct drive of ship's steering gears: concept and FEM analysis", in *Proc. of 22nd Intl. Conference on Electrical Machines (ICEM)*, Marseille, France, Sept. 2-5, 2012, pp. 556-562.
- [4] G. Sulligoi, A. Vicenzutti, R. Menis, "All electric ship design: from electrical propulsion to integrated electrical and electronic power systems", *IEEE Transactions on Transportation Electrification*, vol. 2, issue: 4, pp. 507-521, Dec. 2016.
- [5] N. Doerry, J. Amy, Cy. Krolick, "History and the status of electric propulsion, integrated power systems and future trends in the U.S. Navy", *IEEE Proceedings*, vol. 103, issue 12, pp. 2243-2251, Dec. 2015.
- [6] J.S. Thongam, M. Tarbouchi, F. Okou, D. Bouchard, R. Beguenane, "Trends in naval ship propulsion drive motor technology", in *Proc. of Electrical Power & Energy Conference (EPEC)*, Halifax, NS, Canada, Aug. 21-23, 2013.
- [7] S. Nanoty, A.R. Chudasama, "Design of multiphase induction motor for electric ship propulsion", in *Proc. of IEEE Electric Ship Technologies Symposium (ESTS)*, Alexandria, VA, USA, Apr. 10-13, 2011, pp. 283-287.
- [8] K.I. Nikolaou, M.E. Beniakar, A.G. Kladas, "Design considerations in induction motors for ship thruster propulsion", in *Proc. of Intl. Conference on Electrical Machines (ICEM)*, Berlin, Germany, Sept. 2-5, 2014, pp. 2286-2292.
- [9] T.D. Batzel, K.Y. Lee, "Electric propulsion with the sensorless permanent magnet synchronous motor: model and approach", *IEEE Transactions on Energy Conversion*, vol. 20, no. 4, pp. 818-825, 2005.
- [10] Y.U. Cho, S.L. Lee, G.H. Kang, B.W. Kim, "Design and verification of 200 kW interior permanent magnet synchronous motor for ship propulsion", in *Proc. of IEEE Electromagnetic Field Computation (CEFC)*, Miami, FL, USA, Nov. 13-16, 2016.
- [11] A. Hassannia, A. Darabi, "Design and performance analysis of superconducting rim-driven synchronous motors for marine propulsion", *IEEE Transactions on Applied Superconductivity*, vol. 14, no. 1, Feb. 2014. DOI: 10.1109/TASC.2013.2280346.
- [12] T. Yanamoto, M. Izumi, K. Umamoto, T. Oryu, Y. Murase, M. Kawamura, "Load test of 3-MW HTS motor for ship propulsion", *IEEE Transactions on Applied Superconductivity*, vol. 27, no. 8, Dec. 2017. DOI: 10.1109/TASC.2017.2754270.
- [13] M. El-Refaie, "Motors/generators for traction/propulsion applications: a review", *IEEE Vehicular Technology Magazine*, vol. 8, issue 1, pp. 90-99, Mar. 2013.
- [14] H. Karmaker, D. Sarandria, M. T. Ho, J. Feng, D. Kulkarni, G. Rupertus, "High-power dense electric propulsion motor", *IEEE Transactions on Industry Applications*, vol. 51, no. 2, pp. 1341-1347, 2015.
- [15] A. Kasha, R. Lin, S. Sudhoff, J. Chalfant, J. Alsawalhi, "A comparison of permanent magnet machine topologies for marine propulsion applications", in *Proc. of IEEE Symposium on Electric Ship Technologies (ESTS)*, Arlington, VA, USA, Aug. 14-14, 2017.
- [16] H.Y. Choi, S.J. Park, Y.K. Kong, J.G. Bin, "Design of multi-phase permanent magnet motor for ship propulsion", in *Proc. of Intl. Conference on Electrical Machines and Systems (ICEMS)*, Tokyo, Japan, Nov. 15-18, 2009.
- [17] M. Qiao, C. Jiang, Y. Zhu, G. Li, "Research on design method and electromagnetic vibration of six-phase fractional-slot concentrated-winding PM motor suitable for ship propulsion", *IEEE Access*, vol. 4, pp. 8535 - 8543, 2016.
- [18] J.H. Paulides, N. Djukic, L. Encica, "Hybrid shipping for inland navigation: loss analysis of an aluminum direct-drive high performance 11,000 Nm permanent magnet machine", in *Proc. of 10th Intl. Conference on Ecological Vehicles and Renewable Energies (EVER)*, Monte Carlo, Monaco, Mar. 31- Apr. 2, 2015.
- [19] R.J. Thome, E. Bowles, M. Reed, "Integration of electromagnetic technologies into shipboard applications", *IEEE Transactions on Applied Superconductivity*, vol. 16, no. 2, pp. 1074-1079, 2006.
- [20] S.Y. Kim, Y.D. Yoon, S. Ki Sul, "Suppression of thrust loss for the maximum thrust operation in the electric propulsion ship", *IEEE Transactions on Industry Applications*, vol. 45, no. 2, pp. 756-762, Mar. 2009.
- [21] P. Michalopoulos, F.D. Kanellos, G.J. Tsekouras, J.M. Prousalidis, "A method for optimal operation of complex ship power systems employing shaft electric machines", *IEEE Transactions on Transportation Electrification*, vol. 2, issue 4, 2016, pp. 547-557, Dec. 2016.
- [22] S.K. Lee, G.H. Kang, Jin Hur, "Finite element computation of magnetic vibration sources in 100 kW two fractional-slot interior permanent magnet machines for ship", *IEEE Transactions on Magnetics*, vol. 48, no. 2, pp. 867-870, Jan. 2012.
- [23] G. Sarigiannidis, A.G. Kladas, A. Mountaneas, M.E. Beniakar, G. Politis, I.K. Pallis, E.C. Tatakis, S.E. Dallas, J.M. Prousalidis, "Design of surface PM motors for Pod application utilizing a 3D hydrodynamic model", in *Proc. of 22th Intl. Conference on Electrical Machines (ICEM)*, Lausanne, Switzerland, Sept. 4-7, 2016.
- [24] Y.L. Karnavas, I.D. Chasiotis, C. Korkas, S. Amoutzidis, "Modelling and multiobjective optimization analysis of a permanent magnet synchronous motor design", *International Journal of Numerical Modelling, Electronics Networks, Devices and Fields*, vol. 30, issue 6, Dec. 2017. DOI: 10.1002/jnm.2232.
- [25] "System Project Guide for Passenger Vessels", ABB, Available: https://library.e.abb.com/public/608df0ae42ea2ce8c1257abd004ff506/ABB_System_Project_Guide_Passenger_Vessels.pdf, (access on 25-02-2018).
- [26] J.J. Choi, Y.D. Chun, P.W. Han, M.J. Kim, D.H. Koo, J. Lee, J.S. Chun, "Design of high power permanent magnet motor with segment rectangular copper wire and closed slot opening on electric vehicles", *IEEE Transactions on Magnetics*, vol. 46, issue 6, pp. 2070-2073, Jun 2010.
- [27] T. Ishigami, Y. Tanaka, H. Homma, "Development of motor stator with rectangular-wire lap winding and an automatic process for its production", *Electrical Engineering in Japan*, Wiley, vol. 187, issue 4, pp. 51-59, Jun. 2014.
- [28] J. Robinson and Y. Rahmat-Samii, "Particle swarm optimization in electromagnetics", *IEEE Transactions on Antennas and Propagation*, vol. 52, no. 2, pp. 397-407, Feb. 2004.

VII. BIOGRAPHIES

I. D. Chasiotis was born in Athens, Hellas, 1991. He received the Diploma Degree in electrical and computer engineering from the Department of Electrical and Computer Engineering (DECE), Democritus University of Thrace (DUTH), Xanthi, Hellas. He is with the Electrical Machines Laboratory of the same Department where he is currently pursuing his PhD degree. His research interests are in the area of electrical machines design, the incorporation of optimization methods in the design process and the development of permanent magnets synchronous and induction machines with characteristics of high power density and high efficiency. He has gained a full time award scholarship from Onassis Foundation for his post-graduate studies. He is a member of Hellenic Technical Chamber and student member of IEEE.

Y. L. Karnavas was born in Volos, Hellas, 1969. He received the Diploma Degree and his PhD from the Department of Electrical and Computer Engineering (DECE), Democritus University of Thrace (DUTH), Xanthi, Hellas in 2002. He is with the Electrical Machines Laboratory of the DECE, DUTH as an Assistant Professor. His research interests include electrical machines design, analysis, modeling and optimization, controller design and application to electrical machines and artificial intelligence methods application to them. He has published several papers in various international journals and conferences, as well as book chapters in international engineering books. He has participated in many research projects as research leader or scientific associate. He serves as an Associate Editor and as an Editorial board member in various international scientific journals. He is a chartered electrical engineer as well as a member of Hellenic Technical Chamber. Prof. Karnavas is also an IEEE, IEEE PES, IEEE IAS and IEEE IES member.